energies

MDPI

Article

A Novel Robust Model Predictive Controller for Aerospace Three-Phase PWM Rectifiers

Tao Lei *, **Weiwei Tan**, **Guangsi Chen** and **Delin Kong**

Key laboratory of Aircraft Electric Propulsion Technology, Ministry of Industry and Information Technology of China, Northwestern Polytechnic University, Xi'an 710072, China; Tanww1994@163.com (W.T.); chenguangsi@mail.nwpu.edu.cn (G.C.); kline@mail.nwpu.edu.cn (D.K.)

* Correspondence: lttiger@nwpu.edu.cn

Received: 24 August 2018; Accepted: 14 September 2018; Published: 19 September 2018

Abstract: This paper presents a novel Model Predictive Direct Power Control (MPDPC) approach for the pulse width modulation (PWM) rectifiers in the Aircraft Alternating Current Variable Frequency (ACVF) power system. The control performance of rectifiers may be largely affected by variations in the AC side impedance, especially for systems with limited power volume system. A novel idea for estimating the impedance variation based on the Bayesian estimation, using an algorithm embedded in MPDPC is presented in this paper. The input filter inductance and its equivalent series resistance (ESR) of PWM rectifiers are estimated in this algorithm by measuring the input current and input voltage in each cycle with the probability Bayesian estimation theory. This novel estimation method can overcome the shortcomings of traditional data based estimation methods such as least square estimation (LSE), which achieves poor estimation results with the small samples data set. In ACVF systems, the effect on the parameters estimation accuracy caused by the number of sampling points in one cycle is also analyzed in detail by simulation. The validity of this method is verified by the digital and Hard-in-loop simulation compared with other estimation methods such as the least square estimation method. The experimental testing results show that the proposed estimation algorithm can improve the robustness and the control performance of the MPDPC under the condition of the uncertainty of the AC side parameters of the three-phase PWM rectifiers in aircraft electrical power system.

Keywords: Model Predictive Direct Power Control (MPDPC); Aircraft Electrical Power System; PWM rectifiers; Bayesian estimation methods

1. Introduction

In the recent years, thanks to technological advances in microprocessors, model predictive control (MPC) has been proposed and studied as a promising alternative for the control of power converters and drives [1]. This control strategy has been used for inverter [2], rectifier [3,4], active power filter [5] and Uninterrupted Power Supply (UPS) [6]. In aircraft electrical power system, the pulse width modulation (PWM) rectifiers have more advantages than the traditional multi-pulse Transformer/Autotransformer-Rectifiers (TRU or ATRU) applied in the aircraft electrical power system, such as the regulated DC voltage and high power factor in the AC side [7]. In the aircraft electrical power system, the limitation about the total harmonic distribution (THD) of AC input current is very strict about less than 10% [8]. Based on a mathematical model of PWM rectifiers, and predicting the possible future controlling input variables, the Finite Control Set-Model Predictive Control (FCS-MPC) [9] achieves numerous similar performance including the high power factor and sinusoidal input currents with little harmonic pollution compared with other traditional control methods in the aircraft electrical power system. Furthermore, the advantages of MPC within PWM rectifiers are the abilities to handle constraints, multiple inputs and outputs and nonlinearities in a simple and intuitive manner.

A commonly used MPC control algorithm for three-phase PWM rectifiers is Model Predictive Direct Power Control (MPDPC) [10–14]. The input active power and reactive power in DPC are controlled by measuring input AC current. The three-phase bridge leg corresponds to eight possible switching states and eight possible input current states. Finally, the cost function is used to evaluate the eight switching states and select the best switching vector in the next cycle. The control performance of the FSC-MPC depends on the accurate predictions of the future state. Mismatches between the parameters used in the model and the actual parameters of PWM rectifiers may result in inaccurate selection of the optimal control vector. Inaccurate system models can cause some degradation in control performance. This issue is very important for the MPC applied to the aerospace PWM rectifier, which makes the system potentially susceptible to the mismatches from the temperature and environmental effect.

Recently, in order to solve the problem of uncertainty of model parameters, several estimation methods with MPC are suggested. These methods can be classified into the model based estimation methods and data based methods. Paper [15] proposed a parameter estimation method based on least square estimation (LSE). These methods belong to data based methods and the LSE methods just are applied to the 50 Hz power system in this paper. The least square method is applied to accurately estimate the inductance value but the response of this estimator will become slow with an increase of the program runtime. A MPDPC control with the inductance parameters compensation methods is applied to the single phase three-level rectifiers [16]. The research is focused on low switching frequency from 1–20 KHz, it is naturally data based methods.

The MPC with the model based estimation methods also has been widely researched. Paper [17] proposed a kind of adaptive robust observer based on direct torque control for the field of AC motor drive but it is not prevalently studied in the three-phase PWM rectifier. In Reference [18], Based on a three-phase PWM rectifier, a robust model predictive control algorithm with disturbance observer is proposed. The influence of model parameter mismatch on the system is regarded as a perturbation and the Luenberger observer is used to eliminate system disturbances by feed-forward compensation and enhance the stability of the control system. Nevertheless, many parameters of observer need to be tuned in this algorithm and it is complicated in the process of designing Luenberger observer. A non-linear constrained control strategy based on robust model prediction and sliding mode control with the parameter estimation is proposed in Reference [19]. However, this method is not applicable to referring to discrete-time model of PWM rectifiers, which is only designed for continuous-time model. Paper [20] combined the MPDPC with the sliding mode Observer in PWM rectifiers under unbalanced grid conditions. The voltage sensor-less control can be realized by the observer and the error of parameters variation is compensated in a satisfied range. This method is only verified in 50 Hz power system. The extended Kalman-Filter with online grid impedance estimation was proposed for the control of grid connected converter in Reference [21], these control algorithms also belong to the model based methods, the ground grid impedance model was derived based on the rectifiers' model. But the complexity of rectifier's model with observer was only verified by simulation. The tuning of the covariance matrices of the extended kalman filter (EKF) is based on trial-and-error procedure.

In additional, the grid-side online impedance estimation methods based on the power relationship and voltage vector relationship were presented respectively in Reference [22–26], these methods only consider the ground grid connected converter situation, the parameters of grid network changed largely and the control methods with parameter estimation is not limited to the MPC control. The Uncertainty of parameters of PWM rectifiers in ACVF electrical power system cannot be investigated, the characteristics of ac side impedance parameters changed with main AC generator frequency with the load profile. So, the research topic about the aerospace PWM rectifiers with MPDPC control under parameter uncertainty is very significant. Compared with the model based methods, the parameters estimation methods from the data based are easily accomplished by the MPC controller by measuring the input and output measurement data to estimating the AC side of the inductor parameters to make it sure that the rectifier model parameters and the actual circuit parameters are kept same in real time. So, the data based estimation method with the MPDPC is the topic of focus in this paper.

The main frequency may suffer obvious variations as high as 100%, depending upon the power consumption in the aircraft electrical power system [27]. The main frequency can be changed from the 360–800 Hz and this further deteriorates control performance of MPDPC. Based on the aerospace three-phase PWM rectifier, the cause and influence of inaccurate input filter inductance's variation are discussed in this paper. MPDPC with Bayesian estimation algorithm is proposed to estimate the actual value of inductance in limited samples data set. The shortcomings of slow convergence rate and instability for the estimated value are overcome by this method compared with the LSE methods proposed in Reference [15]. The realization of control algorithm does not require additional sensors and can be implemented directly in the digital microprocessor. The main contributions of this work include the following:

1. A MPDPC with the Bayesian estimation for PWM rectifiers in the aircraft ACVF power system is presented, which has not been fully investigated in existing literature for PWM rectifier's parameter estimation. The probability distribution function of estimated parameters is presented through the analysis of variation for inductance's value caused by different factors such as temperature. The Bayesian estimation algorithm integrated with MPDPC is derived in detail.
2. The performance of the Bayesian estimation is compared with LSE according to the converging rate, stability of estimated parameters by digital simulation. For the Bayesian methods with MPDPC, the result of the estimation is also compared by using the input current signal with white noise. The digital simulation results validate the robust of Bayesian estimation to disturbance from the input signals. From the numbers of samples for the input measuring signal, The Bayesian estimation methods do not need more samples which would greatly reduce the computational complexity.
3. The proposed Bayesian estimation method is compared with the LSE method and traditional MPDPC in experiments. The advantage of estimation methods is verified by digital simulation and experimental results. The several performance indexes are listed in following Tables to be discussed, the final conclusion can be obtained to test the feasibility of the proposed method.
4. The Hard In Loop (HIL) and experimental testing rig was built to verify the theoretical analysis under the aircraft ACVF Power system.

The remainder of this paper is organized as follows. The basic operation theory of MPDPC is introduced in Section 2. The realization of an online parameter estimation algorithm based on Bayesian estimation with the MPDPC is proposed in Section 3. Digital simulation and semi-physical experiment results are shown in Section 4 and the hardware prototype experiments is carried out in Section 5. The conclusion is discussed in Section 6 and the detail derivative process of Bayesian estimation method is elaborated in Appendix A.

2. Traditional Model Predictive Control Algorithm

The three-phase PWM rectifier mainly consists of input filter inductor, Insulated Gate Bipolar Transistor (IGBT) Rectifier Bridge and output filter capacitor. The input power and output voltage are controlled by traditional MPC algorithm through controlling the switch state of IGBTs. A typical three-phase PWM rectifier topology is shown in Figure 1.

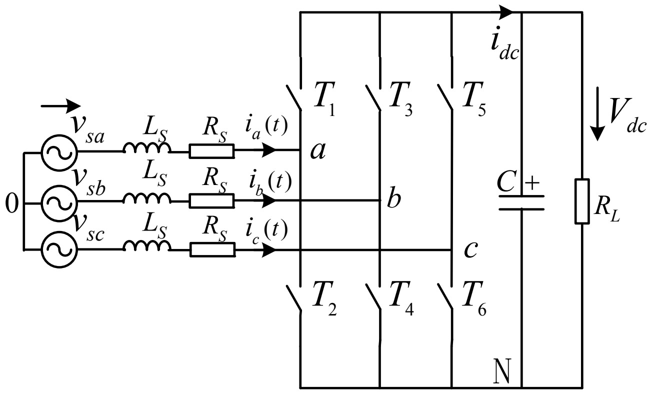

Figure 1. The topology of three-phase pulse width modulation (PWM) rectifier.

The three-phase input voltage v_s, input current i_s and PWM rectifiers bridge voltage v_{REC} are expressed in $\alpha\beta$ orthogonal coordinates as (1)–(3), respectively.Note that the rectifier bridge voltages are expressed with the dc-link voltage and the switching functions:

$$v_s = \frac{2}{3}(v_{sa} + v_{sb}e^{j(2\pi/3)} + v_{sc}e^{j(4\pi/3)}) \tag{1}$$

$$i_s = \frac{2}{3}(i_{sa} + i_{sb}e^{j(2\pi/3)} + i_{sc}e^{j(4\pi/3)}) \tag{2}$$

$$v_{REC} = \frac{2}{3}(s_a + s_b e^{j(2\pi/3)} + s_c e^{j(4\pi/3)})V_{dc} \tag{3}$$

where s_a, s_b, s_c are the switching states of the three-phase rectifier bridge upper switch take on the binary values of "1" and "0" in the closed state and open state, respectively. The relationship of the input and output of a three-phase PWM rectifier system is expressed in vector form as:

$$L_s \frac{di_s}{dt} = v_s - v_{REC} - R_s i_s \tag{4}$$

By approximating the derivative of the inductance currents on the basis of the forward Euler approximation with a sampling period T_s, the three-phase PWM rectifier system in the continuous-time model will be represented in the discrete-time domain as:

$$i_s(k+1) = (1 - \frac{R_S T_S}{L_S})i_s(k) + \frac{T_S}{L_S}[v_s(k) - v_{REC}(k)] \tag{5}$$

In order to solve the computational delay in the model prediction algorithm, two-step prediction is performed, which is shifting the inductance current in (5) by one step forward, so the inductance current is represented as:

$$i_s(k+2) = (1 - \frac{R_S T_S}{L_S})i_s(k+1) + \frac{T_S}{L_S}[v_s(k+1) - v_{REC}(k+1)] \tag{6}$$

The input voltage at the next time $k+1$ instant can be assumed to be equal to the sampling value at the k instant, based on the assumption that the sampling frequency is much larger than the main frequency of the aircraft electrical power system, According to the instantaneous power calculation methodin Reference [28], the future instantaneous input real and reactive powerare presented as:

$$P(k+2) = i_{s\alpha}(k+1)v_{s\alpha}(k+1) + i_{s\beta}(k+1)v_{s\beta}(k+1) \tag{7}$$

$$Q(k+2) = i_{s\alpha}(k+1)v_{s\beta}(k+1) + i_{s\beta}(k+1)v_{s\alpha}(k+1) \tag{8}$$

The common cost function of MPDPC is the error between the value of prediction and reference of active and reactive power.

$$g_{DPC} = \left|P_{ref} - P(k+1)\right| + \left|Q_{ref} - Q(k+1)\right| \tag{9}$$

3. Online Parameter Estimation Algorithm

As shown in (5) and (6), the rate of AC input current change is affected by the inductance value directly. Meanwhile, the uncertainty of model parameters will affect the accuracy of predicted active and reactive power, so the selection of the optimal switching states and the system performance also will be disturbed eventually.

As shown in Figure 2, assuming that the reference value of active power P_{ref} is a constant, and $P(t)$, $P_m(t)$ represent the actual value and the predicted value of the active power, respectively. According to the sampling progress, there is a deviation between the actual value of active power $P(t_k)$ and the predicted value $P_m(t_k)$ at the sampling time t_k Then, at the sampling time t_{k+1}, the optimal switching vector S_3 is selected on the basis of the predicted active power value $P_m(t_{k+1})$ and the given reference value of active power P_{ref}. Thus, the actual value of the active power obtained is $P(t_{k+2})$, which has already deviate from the reference P_{ref}. So, it should be S_5 not S_3 is the optimal switching vector for $P(t_{k+1})$. Errors in model parameters lead to errors between the predicted and the reference value of the active and reactive power and result in inaccurate prediction results, meanwhile, affect the harmonic content of the AC side current, even reduce the performance of the three-phase rectifier system.

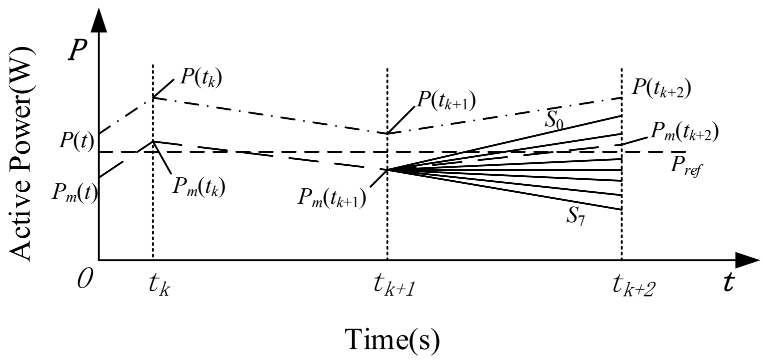

Figure 2. Power prediction under the influence of model parameter errors.

In order to improving the steady state performance of three-phase PWM rectifier, realizing the unity power factor and reducing the harmonic content of AC current, an online parameter estimation algorithm based on Bayesian estimation is proposed with MPDPC.

The input current of (6) is transformed as:

$$i_s(k+1) = \lambda i_s(k) + \mu[v_s(k) - v_{REC}(k)] \tag{10}$$

where

$$\lambda = 1 - \frac{R_s T_s}{L_s} \tag{11}$$

$$\mu = \frac{T_s}{L_s} \tag{12}$$

Based on the (10), the α-axis component of the input current i_s, input voltage v_s and rectifier bridge voltage v_{REC} at stationary coordinate, can be represented as:

$$i_{s\alpha}(k+1) = \lambda i_{s\alpha}(k) + \mu[v_{s\alpha}(k) - v_{REC\alpha}(k)] + \nu + \varepsilon(k) \tag{13}$$

where the v and $\varepsilon(k)$ represent DC bias and error during measurement respectively. The $(k-1)$th equations constructed with the $(k-1)$ successive sampled data points in (13) are used and rewritten in matrix form as:

$$\begin{bmatrix} i_{s\alpha}(2) \\ \vdots \\ i_{s\alpha}(k) \end{bmatrix} = \begin{bmatrix} i_{s\alpha}(1) & v_{s\alpha} - v_{REC\alpha}(1) & 1 \\ \vdots & \vdots & \vdots \\ i_{s\alpha}(k-1) & v_{s\alpha}(k-1) - v_{REC\alpha}(k-1) & 1 \end{bmatrix} \begin{bmatrix} \lambda \\ \mu \\ v \end{bmatrix} + \begin{bmatrix} \varepsilon(1) \\ \vdots \\ \varepsilon(k-1) \end{bmatrix} \tag{14}$$

For simplicity, (14) is written in matrix notation as:

$$\mathrm{Y} = \Phi\theta + \varepsilon \tag{15}$$

where

$$\mathrm{Y} = \begin{bmatrix} i_{s\alpha}(2) \\ \vdots \\ i_{s\alpha}(k) \end{bmatrix} \tag{16}$$

$$\Phi = \begin{bmatrix} i_{s\alpha}(1) & v_{s\alpha}(1) - v_{REC\alpha}(1) & 1 \\ \vdots & \vdots & \vdots \\ i_{s\alpha}(\mathrm{k}-1) & v_{s\alpha}(\mathrm{k}-1) - v_{REC\alpha}(\mathrm{k}-1) & 1 \end{bmatrix} \tag{17}$$

$$\theta = \begin{bmatrix} \lambda \\ \mu \\ \nu \end{bmatrix}, \varepsilon = \begin{bmatrix} \varepsilon(1) \\ \vdots \\ \varepsilon(k-1) \end{bmatrix} \tag{18}$$

In (15), Y and Φ are known data that both can be measured. The coefficient θ is to be estimated parameter vector. The paper [15] gives the LSE methods but this method cannot achieve the good performance in small samples data set. The following Figure 3a gives the characteristic of power inductor value of inductance changed with load current and Figure 3b shows that the permeability of iron magnetic materials also changed with different temperature. Because of complexity for the variation of inductance value, So the relationship between variation of inductance and the current, temperature is nonlinear relationship. It is very difficult to describe the relationships with accurate analytical equation [29]. Through the data statistics processing procedure from the curve of inductance, the estimated parameters such as inductance value are assumed to follow the normal distribution around variation of inductance. The Figure 4a presents the histogram of inductance value which has been changed in different currents and temperatures. In the Figure 4a, the f_k describing how often such result or values happened. So, Figure 4b presents the probability density function, which can describe the distribution of the inductance value. it is related to the histogram for infinite number of measurements for the inductance (continuous function approximation) while the cumulative distribution function is related to cumulative histogram.

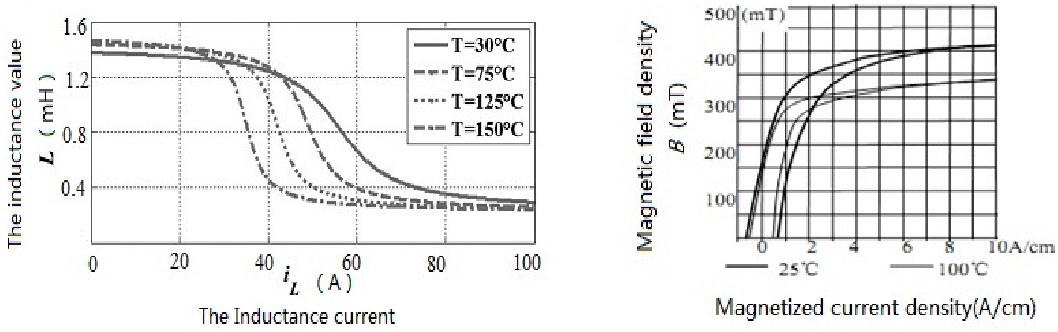

(a) (b)

Figure 3. The characteristics of (**a**) inductance changed with the currents and (**b**) permeability of the iron magnetic material under different temperatures.

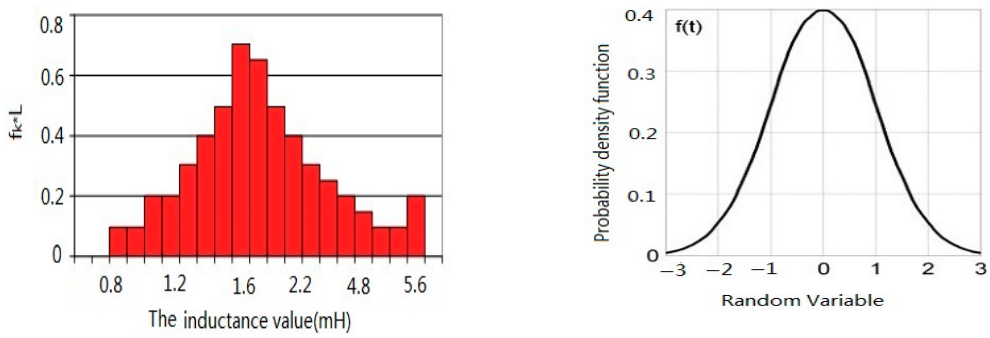

(a) (b)

Figure 4. The histogram of the inductance value (**a**) and probability density distribution function (**b**).

According to the above analysis, the priority distribution function of the estimation parameters can be expressed by the Gaussian function. Based on Bayesian estimation theory in Reference [30], the estimation formula of coefficient θ is shown as (19). Specific detailed formula derivation process is shown in the appendix. The following equation is same as the formula (17) in the appendix.

$$\hat{\theta}_B = (\mathrm{E} + \Phi'\Phi)^{-1}(\mu_0 + \Phi'\Phi\hat{\theta}) = (\mathrm{E} + \Phi'\Phi)^{-1}(\mu_0 + \Phi'\mathrm{Y}) \tag{19}$$

where

$$\hat{\theta}_B = \begin{bmatrix} \hat{\lambda}_B \\ \hat{\mu}_B \\ \hat{v}_B \end{bmatrix} = \begin{bmatrix} 1 - \frac{R_s T_s}{L_s} \\ \frac{T_s}{L_s} \\ v \end{bmatrix} \tag{20}$$

Bayesian estimation formula of the resistance, inductance and DC bias are shown as:

$$\begin{cases} \hat{R}_{s,B} = \frac{1-\hat{\lambda}_B}{\hat{\mu}_B} \\ \hat{L}_{s,B} = \frac{T_s}{\hat{\mu}_B} \\ \hat{v}_B = \hat{v}_B \end{cases} \tag{21}$$

The consistency of model parameters and the actual circuit parameterswill be guaranteed by taking the estimated coefficient obtained at the end of each sampling time into the original model of the rectifier by using the Equation (19), this can be expressed by Equation (22):

$$i_s(k+1) = \hat{\lambda} i_s(k) + \hat{\mu}[v_s(k) - v_{REC}(k)] \tag{22}$$

For convenience, $\hat{\theta}_B$ can be easily calculated by introducing two dummy matrices A and B as the

$$\hat{\theta}_B = (E + \Phi'\Phi)^{-1}(\mu_0 + \Phi'\mathrm{Y}) = (E + A)^{-1}(\mu_0 + B) \tag{23}$$

where the E denotes the identity matrix. μ_0 denotes the expectation of the coefficient θ.

$$A = \Phi'\Phi = \begin{bmatrix} a_{11} & a_{12} & a_{13} \\ a_{21} & a_{22} & a_{23} \\ a_{31} & a_{32} & a_{33} \end{bmatrix}, B = \Phi'\Upsilon = \begin{bmatrix} b_1 \\ b_2 \\ b_3 \end{bmatrix}.$$

It is noted that regardless of the amount of measured data, A and B become 3-by-3 and 3-by-1 matrices, respectively, forthe three-phase AFE at all times. As a result, calculating $\hat{\theta}_B$, including the calculation of the inverse of A in (23), can be,without calculation burden, processed on the platform of a common DSP in real systems that are generally used for the three phase rectifiers.Using (19) and (23), all the elements of A and are calculated onthe basis of only the measurement of the input current and the input voltage.

The block diagram of the control algorithm is shown in Figure 5. In this control block diagram, the input AC voltage and input AC current must be measured as the data set for estimation, the output dc voltage also need to be acquired to calculate the reference active power reference value. In this control block diagram, the Bayesian estimation algorithm can be integrated with MPDPC control methods. By using the MPDPC with the proposed Bayesian estimation methods, the PWM driving control signal can be selectedoptimally for the three phase PWM rectifiers.

According to the control block diagram in Figure 5 and derived equation based on Bayesian estimation, the MPDPC methods with the Bayesian estimation algorithm can be expressed by following flow chart shown in Figure 6. Firstly, the AC side input voltage and input AC current of PWM rectifiers are measured in every time instants, then the optimal voltage vector from the last time instants can be applied to the rectifiers. Secondly, the parameters update algorithm based on the Bayesian estimation, the Ac side parameters such inductance and resistance can be updated in real time according to the operational conditions of rectifiers. Thirdly, the DPC control calculation can be carried out, the active power and reactive power can be calculated. Finally, the FCS-MPC control algorithm can be used to select optimal voltage vector from the 8 vectors. The process can be repeated in cycle time of input voltage.

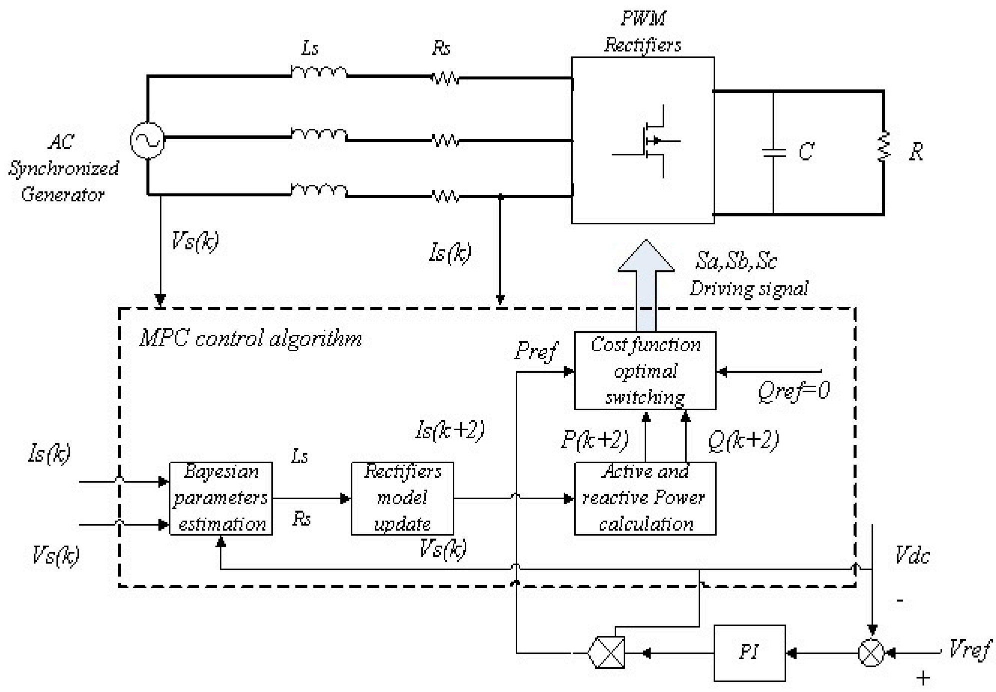

Figure 5. Block diagram of the proposed on-line parameter estimation algorithm with (model Predictive Direct Power Control) MPDPC.

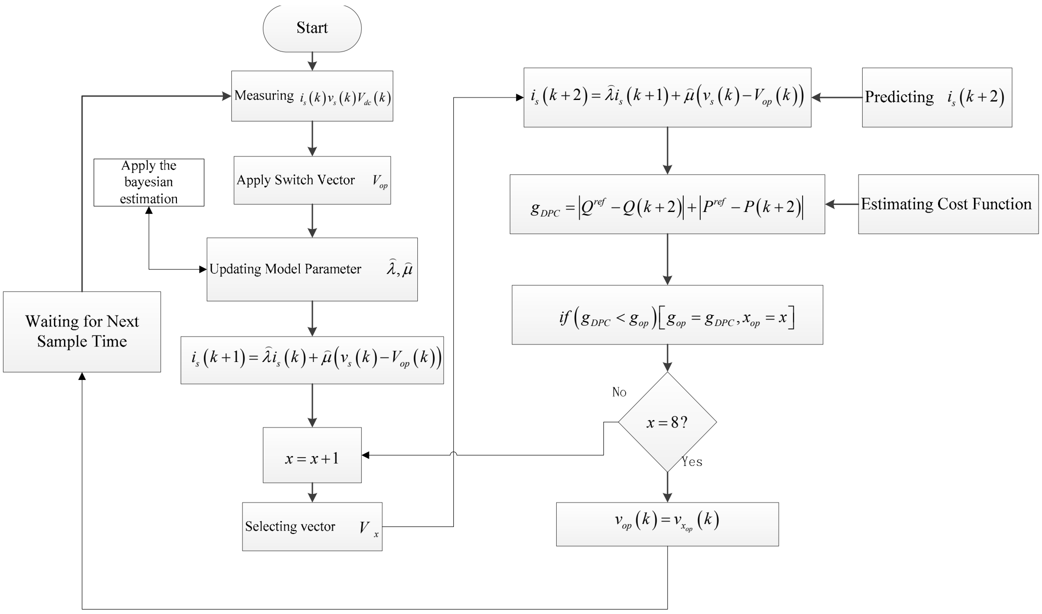

Figure 6. The flow chart of MPDPC control algorithm with Bayesian estimation.

4. Simulation and Experiment Results

4.1. Digital Simulation

According to the on-line parameter estimation algorithm proposed in Section 3, the mathematic simulation model of three-phase PWM rectifier is built in Matlab/Simulink (Matlab R2012, MathWorks, Natick, MA, USA). The algorithm of robust MPDPC is written in S-function. The simulation parameters are shown in Table 1.

Table 1. Digital simulation parameters.

Parameters	Symbol	Value
Input voltage RMS/V	v_{sRMS}	115
Fundamental frequency/Hz	F	400
Sampling period/µs	T_s	20
Output voltage/V	V_{dc}	350
Input inductance/mH	L_s	5
Input resistance/Ω	R_s	0.01
Capacitance/µF	C	940
DC load/Ω	R_L	61.25

With the input inductance L_s changed from 5 mH to 2 mH, the specific simulation results are shown in Figure 7. The input AC current waveform of traditional MPDPC has become distortion and MPDPC with Bayesian estimation algorithm can still guarantee the current sinusoidal. To facilitate the observation of the current waveform, the current waveform has been amplified 10 times. The harmonic components of input current are shown in Figure 8. The total harmonic distribution (THD) of input AC current with traditional MPDPC has reached 23.95% when $L_s = 2$ mH, however the input current's THD has been reduced to 10.57% with Bayesian estimation algorithm applied.

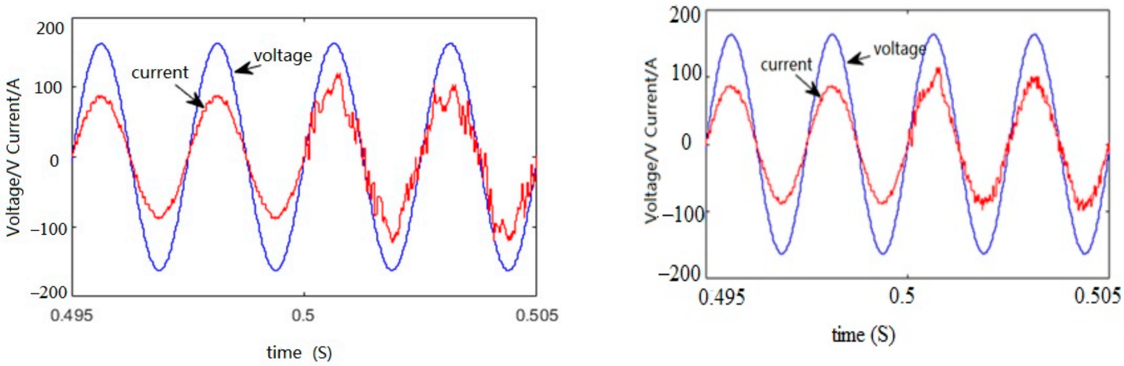

(**a**) (**b**)

Figure 7. AC side voltage and current at inductance parameter changes (**a**) Traditional MPDPC; (**b**) Bayesian estimation algorithm with MPDPC.

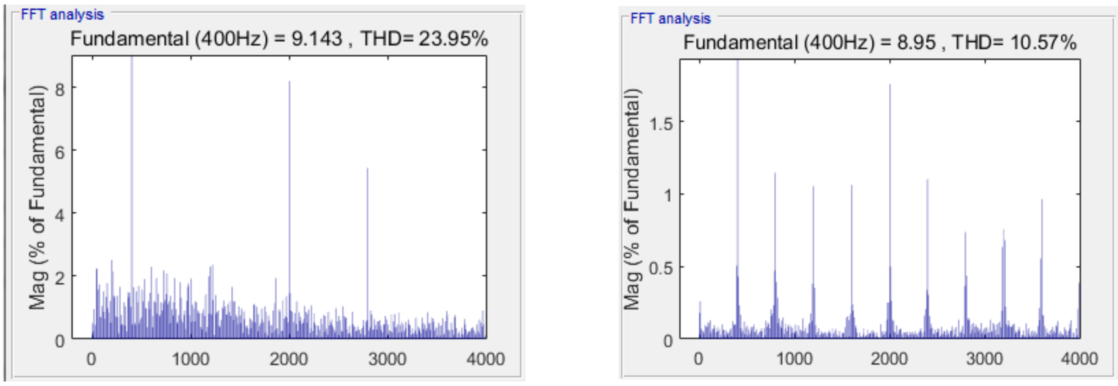

(**a**) (**b**)

Figure 8. The harmonic component of input current. (**a**) Traditional MPDPC; (**b**) MPDPC with Bayesian Estimation Algorithm.

The estimated value of input inductance L_s and input resistance R_s at one sample cycle are shown in Figure 9, with two different parameter data based estimation algorithms: least square method and Bayesian estimation method. When L_s is being changed from the 5 mH to 2 mH quickly, the rate of change of L_s's estimation value in Bayesian estimation is more quickly than it in least square method and the estimated value of L_s keep the same size eventually, with an error about 0.22 mH compared to the simulation given value of L_s. As for the estimated value of R_s, Bayesian estimation indicates faster convergence rate and more stable performance than least square method in limited data samples set.

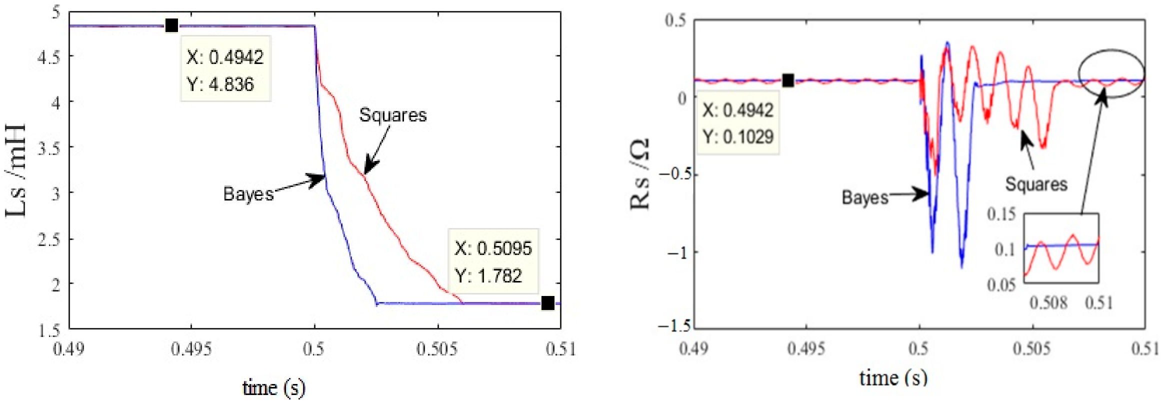

(**a**) (**b**)

Figure 9. The estimated value of L_s and R_s from the different estimation methods. (**a**) Estimated value of L_s; (**b**) Estimated value of R_s.

The application of online parameter Bayesian estimation algorithm depends on the measurement data of input voltage and current. The $k-1$ samples of measuring data from the power converter data are used in the matrix equation in (14). Figure 10 shows the estimated value of L_s and R_s as different samples measurement data chosen with Bayesian estimation. In Figure 10, the 125 samples are the total samples of a full cycle as sampling frequency is 50 KHz and fundamental frequency is 400 Hz. As the chosen samples are total samples of one or more full cycles, the estimated value of L_s and R_s can keepstable. From the Figure 10, it is can be seen that the more the sampling points is in one cycle, the more stable for the estimation value of impedance is, So in ACVF power system, the sampling frequency must be increased to 100 KHz properly by using the Bayesian estimation methods.

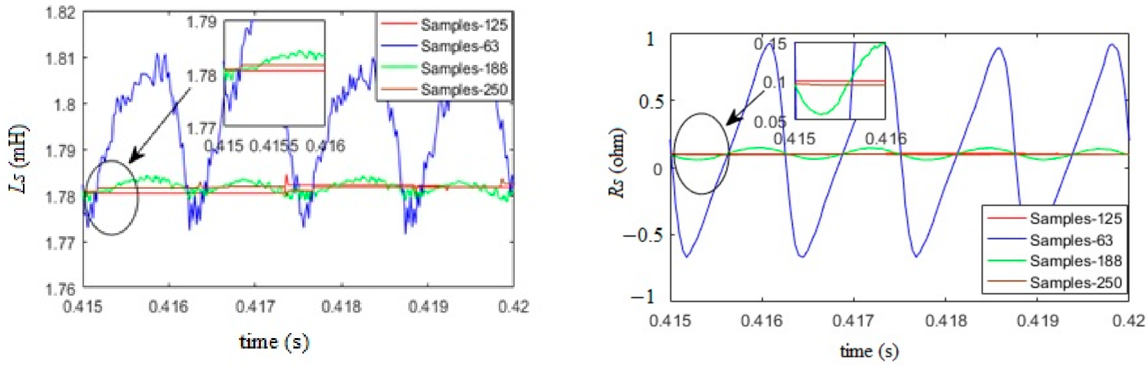

(**a**) (**b**)

Figure 10. The estimated value of and in different samples with Bayesian estimation method ($L_s = 2$ mH, $R_s = 0.1$ Ω) (**a**) Estimated value of L_s; (**b**) Estimated value of R_s.

Figure 11 shows the current harmonic content and power factor when the value of inductance changes. As the inductance parameter decreasing, the online parameter estimation algorithm and least square method can well suppress the rise of current harmonic content and keep the rectifiers operating at high power factor. In the Figure 11, the value of ΔL represents the corresponding value of inductance variation. For instance, $\Delta L = 0.6$ means input inductance is 3 mH as the original inductance value is 5 mH. From the Figure 11, it is concluded that the control performance of PWM rectifiers with data based estimation methods is better than the traditional MPDPC. The Bayesian methods can achieve the same control performance as the LSE method.

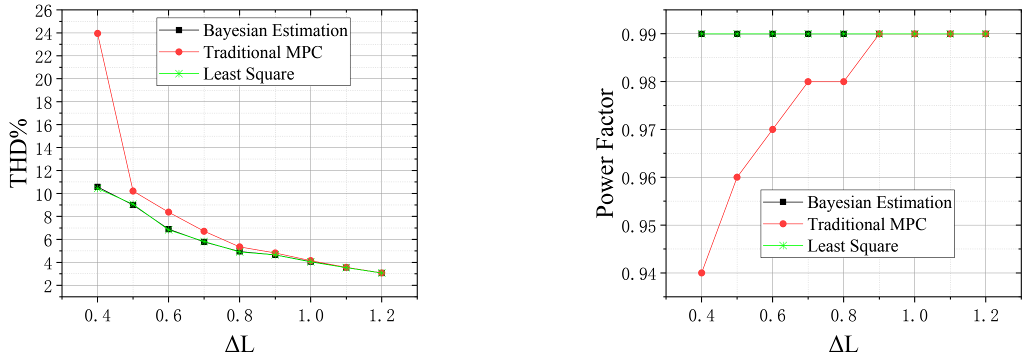

(**a**) (**b**)

Figure 11. Current harmonic content and power factor as inductance parameter changes with different MPDPC methods. (**a**) Current harmonic content under the parameter's variation; (**b**) Power factor under the inductance value's variation.

It us inevitable that the input current which is measured from sensors and ADC (Analog-to-Digital Converter) contains small noises. Figure 12 shows the input current harmonic content with traditional MPDPC, Bayesian estimation and least square algorithms when adding white noise to input AC current signal artificially as inductance parameter changes. As the inductance parameter changes, the THD of input current will increase a little after adding white noise with the measuring current value. Form the Figure 12a, the THD content of input current with Bayesian estimation and LSE with the MPDPC is better than the THD content with the traditional MPDPC under the inductance variation. From the Figure 12b, the robust of control performance with the Bayesian estimation is better than the estimation with LSE when the white noise is added to the input AC current.

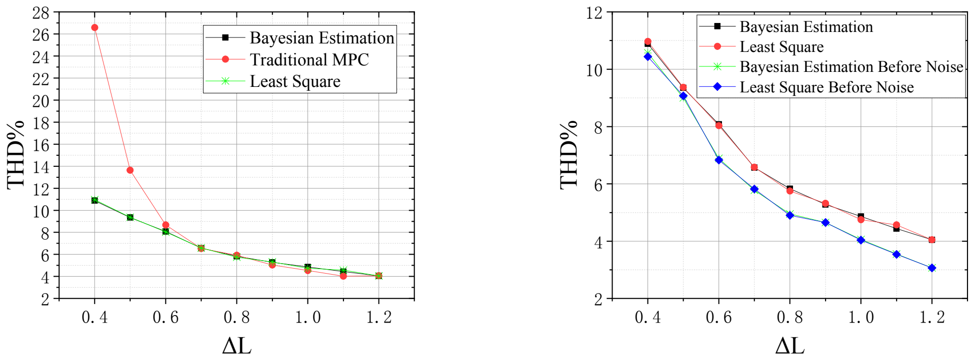

(**a**) (**b**)

Figure 12. THD of current when adding white noise as inductance parameter changes. (**a**) THD of current after adding noise; (**b**) THD of current before and after adding noise.

To verify the dynamic performance of online parameter Bayesian estimation algorithm for load disturbances, an instantaneous load-unload simulation experiment was carried out. The Power reference P_{ref} is from 1000 W to 2000 W and DC load R_L is from 122.5 Ω to 61.25 Ω. Simulation results are shown in Figure 13. Active power has doubled and reactive power is unchanged. The DC bus voltage drops or rises at the moment of loading and unloading but the controller can control the DC voltage back to 350 V. From the Figure 13, the transient dynamics response is achieved by the MPDPC with the Bayesian estimation method.

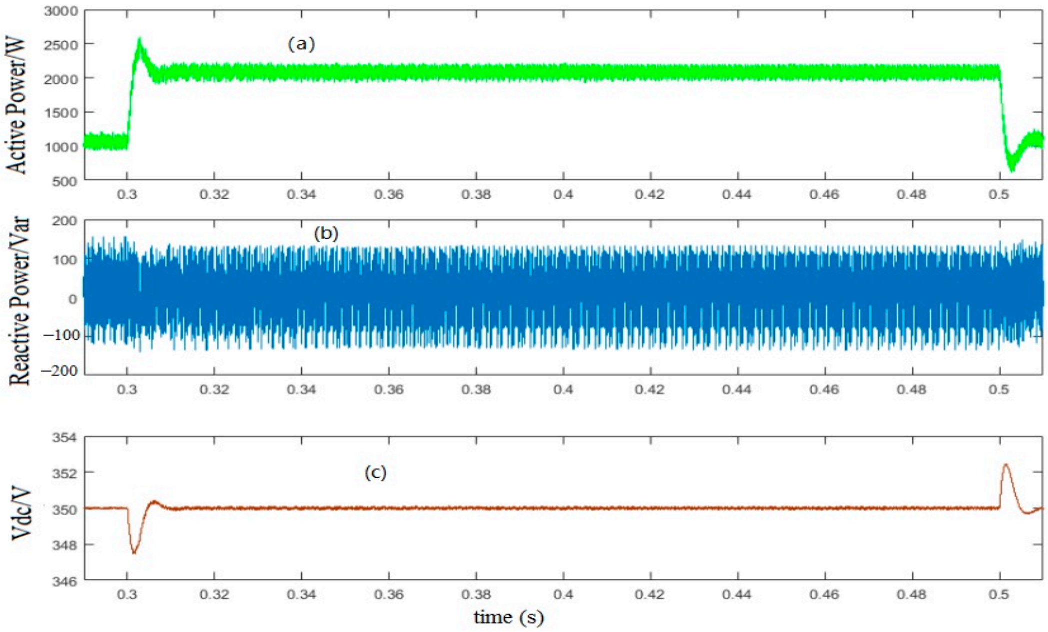

Figure 13. Instantaneous load-unload simulation results by MPDPC with Bayesian estimation method. (**a**) active power; (**b**) reactive power; (**c**) DC bus voltage.

According to the results of digital simulation, the controlling performance of MPDPC with LSE and Bayesian estimation methods is not so different in power factor and THD. But their controlling performance is much better than that of traditional MPDPC's under the variation of parameters of ac side of rectifiers.

4.2. Hard-in-Loop Simulation

At the same time, in order to validate the correctness of the robust MPDPC (RMPDPC) algorithm for the digital simulation platform, a semi-physical test is carried out by the Typhoon-600 semi-physical test platform [31], which is a new and high-fidelity model-based power-electronics testingsystem. The testing system block diagram is shown in Figure 14. The real-time semi-physical test system can achieve simulation time step of 0.1–1 μs, which can provide a test development environment and is closer to the practice operating situation for the aerospace PWM rectifiers. In the Figure 14a, the basic theoretical diagram of HIL is given, The MPDPC control with the Bayesian estimation is programmed in the upper computer. Using the same simulation parameters, the control algorithm is downloadinto the DSP-28335 embedded processor by the Ethernet interface and the aerospace three-phase PWM rectifier model is built on the Typhoon-600 virtual prototype to test control algorithm of RMPDPC for the uncertainty of the inductance parameter. In the Figure 14b, the real hardware configuration with some HIL software are given, through the HIL simulation operation, the simulation waveform can be processed by the analysis software package in the upper computer. In Typhoon platform, the input inductance parameters are easily changed, the controller performance test results shown in Figure 15. From the Figure 15, it is can be seen that the HIL simulation result is very similar with the digital simulation result. The MPDPC with the Bayesian estimation's control performance is better than the traditional MPDPC under the variation of input inductance.

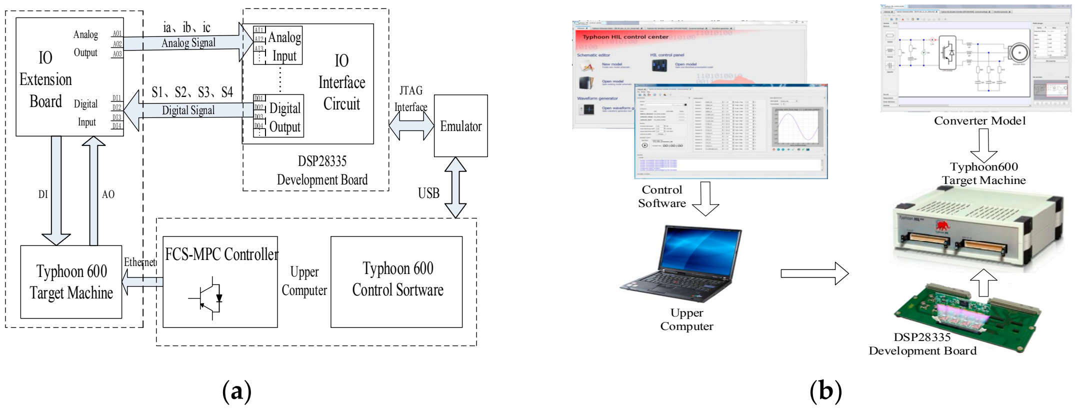

Figure 14. Typhoon semi-physical test platform diagram and practicality. (**a**) The basic theoretical diagram for the HIL system; (**b**) The hardware configuration for the HIL-platform.

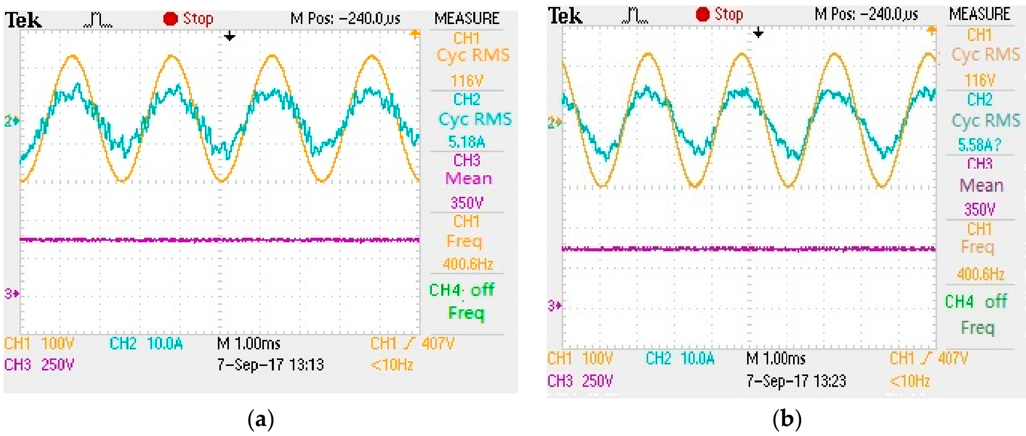

Figure 15. AC side voltage and current at inductance parameter changes (**a**) Traditional MPC (**b**) Online parameter estimation algorithm of MPDPC.

The HIL simulation result of input current's harmonic distortion content and the power factor are shown in Figure 16 when the inductance parameter is changed. In the case of load disturbance, the dynamic performance of the online parameter Bayesian estimation algorithm is verified and the specific HIL experiment results are shown in Figure 17. Both active and reactive power can quickly track the reference value and the voltage of DC bus voltage fluctuates at the moment of loading and unloading but it can be kept constant at 350 V within a short time. The HIL simulation results verified the control effect of MPDPC with the Bayesian estimation methods.

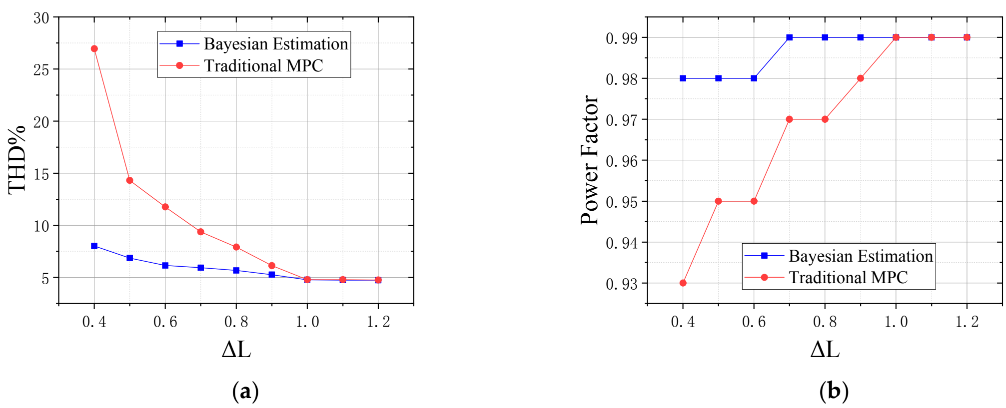

Figure 16. Current harmonic content and power factor in semi-physical test platform under the variation of inductance value. (**a**) AC Current harmonic content; (**b**) AC side Power factor.

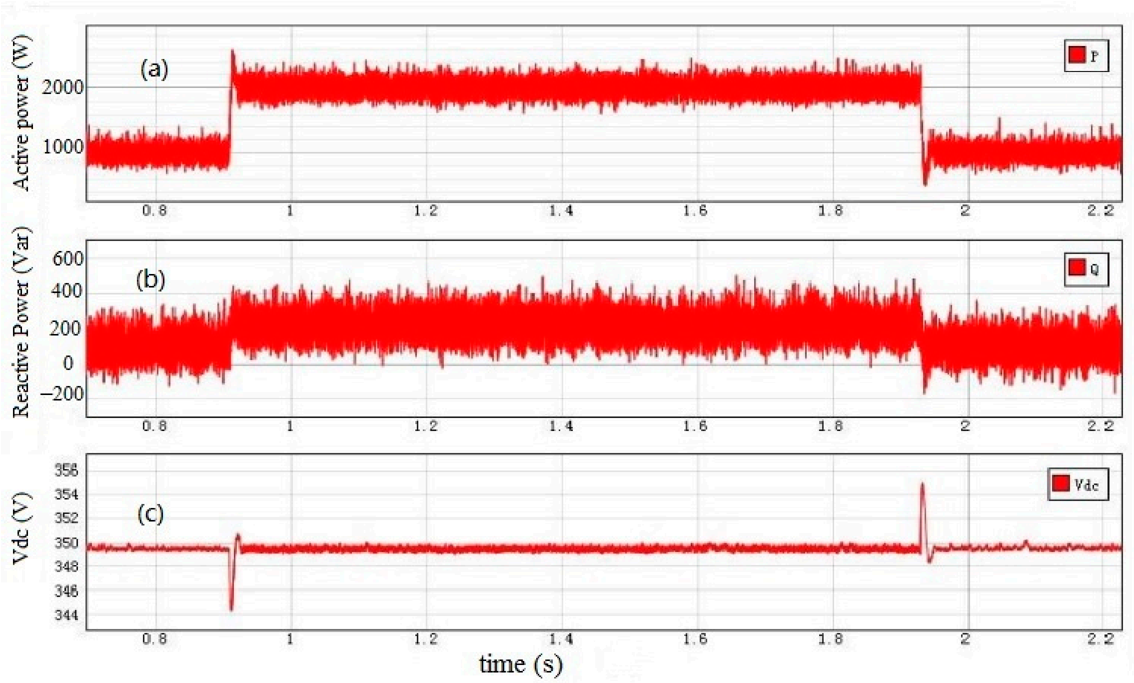

Figure 17. Instantaneous load-unload experiment results. (**a**) Active power; (**b**) Reactive power; (**c**) DC bus voltage.

5. Experimental Verification

The Performance of the designed control system is evaluated on a laboratory test-bench, which is shown in Figure 18. In all test, the Grid voltages and currents are directly measured by probes, while the estimated values of inductance are obtained by a TMS F28335 DSP with sampling frequency 100 KHz. A programmable ac source is used to simulate the aircraft grid conditions. The proposed control scheme is tested in the aircraft electrical power system conditions, in which the input voltage and frequency of PWM Rectifiers is 115 Vrms/360–800 Hz.

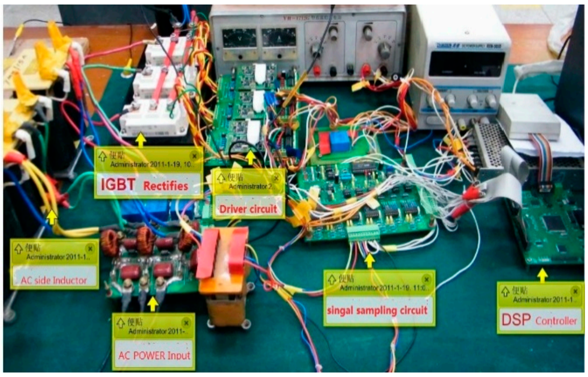

Figure 18. The hardware prototype system.

The prototype AC/DC converter is operating under the normal load for 1 h interval. After that, the values of inductance and resistance can be changed greatly. The Figure 19a, bhighlights the three-phase PWM rectifier's input voltage (red) and input current (green) in phase A by using the Bayesian estimation methods under the variable frequency conditions from the 360 Hz to 800 Hz. The dc-link voltage (blue) can be maintained at the 350 V. So, the controlling performance of PWM rectifiers with the proposed controller can be verified.

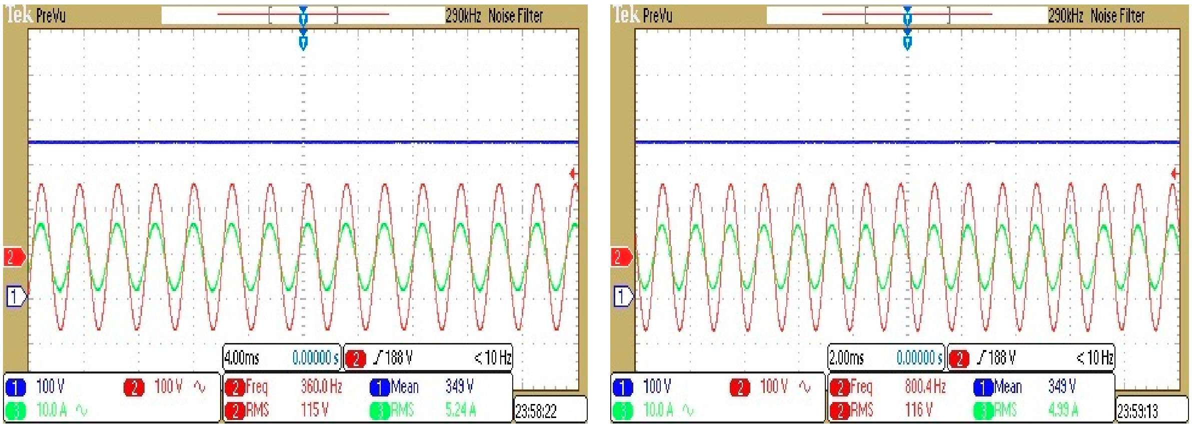

(**a**) (**b**)

Figure 19. The input voltage and current waveform during variable frequency conditions. (**a**) The waveform of rectifiers operated at 360 Hz; (**b**) The waveform of rectifiers operated at 800 Hz.

The Figures 20 and 21 give the experimental result of three-phase PWM rectifiers under the proposal estimation algorithm based on Bayesian methods. According to the experimental result, the output voltage can be regulated to the reference voltage 350 V and input voltage is in same phase with the input current and unity power factor can be realized when the load transient variation and input voltage disturbance happened in aircraft power electrical power system. Figure 20a shows responses for the voltage drop to steady state operation from the 115 Vrms to 80 Vrms and Figure 20 bgives the result of the voltage swell from the 115 Vrms to the 150 Vrms. It is seen that the input current (green) and voltage (red) is in same phase and dc-link voltage (blue) can be kept in constant value at 350 V. These disturbances from the load and power source can make the variable parameters of power circuit such as the input inductance and resistance very serious but the Bayesian estimation algorithm with MPDPC can maintain the better performance. Figure 21a, bprovide the transient waveform for the input voltage (red), current (green) and dc-link voltage (blue) with the load power changed. The results verify the validity of proposed control schemes.

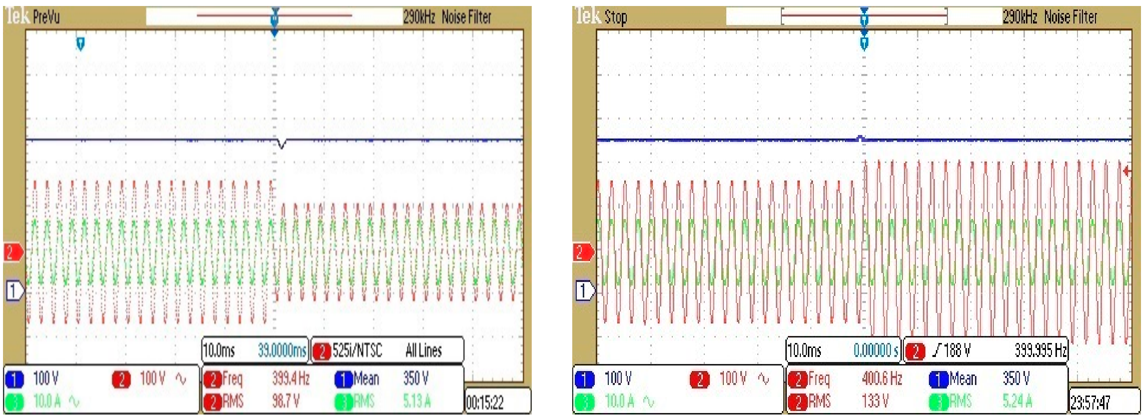

(**a**) (**b**)

Figure 20. The output dc voltage, input voltage and current waveform underthe input voltagetransient variation by the MPDPC with the Bayesian estimation. (**a**) The waveform during input voltage drop; (**b**) The waveform during input voltage swell.

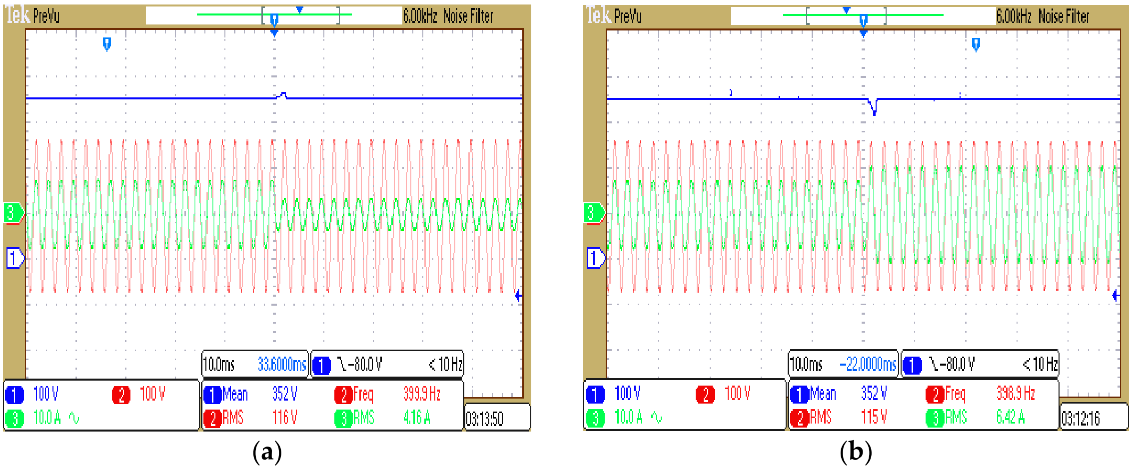

Figure 21. The transient waveforms under the dynamic load power variation. (**a**) The transient waveform of load power from 2.07 KW to 1.08 KW; (**b**) The transient waveform of load power from 1.38 KW to 3.45 KW.

According to the different kinds of MPDPC control scheme, the experimental comparison was carried out. From the result of the THD content of AC input current in Figure 22a, we can infer that the MPDPC controller based on the Bayesian estimation has better performance than other two methods. The variation of inductance can be compensated by the proposal schemes. In Figure 22b, the power factor can be calculated from the input voltage and input current, it is seen that the MPDPC with the Bayesian estimation can achieve the high power factor when the inductance's value changed.

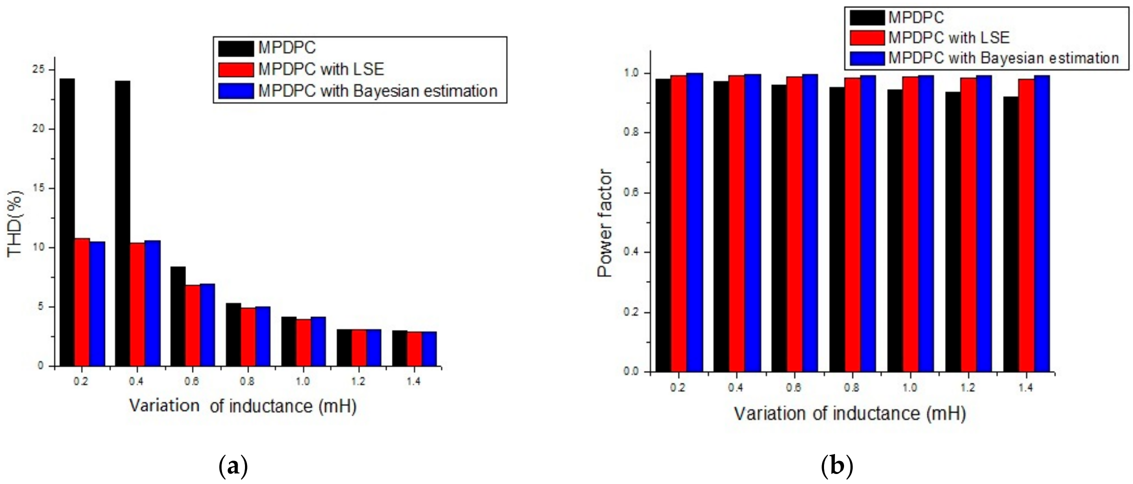

Figure 22. The Bar diagram of performance index under three kinds of MPC control scheme. (**a**) The THD of input current; (**b**) the power factor of rectifiers.

Therefore, the experimental results show the feasibility and the good performance for the proposedrobust model predictive control scheme with fixed sampling frequency in the aircraft electrical power system.

From the above experimental results and theoretical analysis, the performance comparison of three methods applied in three phase rectifier converters can be demonstrated in Table 2, which shows the excellent performance of the proposed methods in the aspects: algorithm complexity, steady state and estimation value dynamics characteristics.

Table 2. Performance Comparison of Three MPC methods under the inductance variation.

Schemes / Performance	Traditional MPDPC	MPDPC with LSE	MPDPC with Bayesian Estimation
Operation time of the algorithm	10.8 uS	15.2 uS	16 uS
THD of line current	8.6%	6.7%	6.8%
Power factor	0.92	0.98	0.99
Converging rate for the estimated value	no	low	fast
Stability for the estimated value	no	low	high

In order to clarify the significance of this research, the experimental results from LSE proposed in the paper [15] are used to be benchmarks for comparison of application in aircraft electricalpower system. The main results and parameters are listed in Table 3. From the comparison in Table 3, it is inferred that the proposed Bayesianmethods also can be applied to the industrial scenario based on the quantitative reasoning. The data set demanding in one cycle based on Bayesian estimation is less than the LSE methods in paper [15].

Table 3. Results and parameters forModel Predictive Direct Power Control (MPDPC) with Bayesian estimation.

Value / Parameters	Results from the Paper [15]	Results from This Paper
Sampling frequency	20 KHz	100 KHz
Main AC Frequency	60 Hz	360–800 Hz
Number of sampling points in one cycle	333	125–270
DC link voltage	260 V	350 V
Rated Power	680 W	1.2 KW
THD of AC current	2.34%	4.68%
Converging time to the true value	10 ms	6.7 ms

6. Conclusions

This paper presents a novel online parameter estimation algorithm for the aerospacethree-phase PWM rectifiers based on Bayesian estimation with MPDPC. In view of the problem that the uncertainty model parameters, the model parameter can be updated every cycle with the proposed algorithm by sampling input Ac current and voltage waveform.With the estimated value of input inductance in each sampling period, the future value of input current, active power and reactive power can be accurately predicted. The problem of controller performance degradation resulted from the uncertainty parameters can be overcome.The successful results of the proposed schemeswere verified by using simulation and experimental test results. It is concluded that the proposed algorithm can reduce the current harmonic contents and improve power factor of PWM rectifiers without additional sensors.Compared with the industrial frequency 50–60 Hz ground power system application, it us also applicable to the aircraft electrical power system. The robust MPDPC based on Bayesian estimation methods can achieved better performance than the LSE-based MPC in small samples data set situation. Using limited small samples data set, The Bayesian methods can estimate the parameters with faster convergence rate and stable value than the result from LSE methods. In the future research, the different priority probability distribution function such as unity distribution or student distribution function can be used to estimate the parameters of AC side for PWM rectifiers. The different results including the accuracy and transient performance of PWM rectifiers can be compared in the Aircraft electrical power system.

Author Contributions: T.L. and W.T. proposed the Bayesian estimation MPC control strategy; W.T. build the simulation model for the three-phase PWM rectifiers converter in aircraft electrical power system; G.C., D.K. and T.L. performed theexperiments for rectifiers converter; W.T. and T.L. analyzed the simulation and experimental data; T.L., W.T. and G.C. wrote the paper.

Conflicts of Interest: The authors declare no conflict of interest.

Nomenclature

A,B	Parameters matrix dimension 3 × 3.
Y	Parameters matrix dimension (k − 1) × 1.
Φ	Parameters matrix dimension (k − 1) × 3.
θ, ε	Estimated parameters matrix (3 × 1) and error matrix [(k − 1) × 1].
λ, μ, ν	Estimated parameters.
v_s	Grid voltage vector $\begin{bmatrix} v_{sa} & v_{sb} & v_{sc} \end{bmatrix}^T$.
i_s	Grid current vector $\begin{bmatrix} i_{sa} & i_{sb} & i_{sc} \end{bmatrix}^T$.
v_{REC}	Voltage vector of PWM rectifiers.
L_s	Grid filter inductance.
R_s	Grid filter resistance.
$v_{s\alpha}, v_{s\beta}$	Grid α, β axis voltage.
$i_{s\alpha}, i_{s\beta}$	Grid α, β axis current.
v_{dc}	rectifiers dc link voltage.
P, Q	Grid active and reactive powers.
P_{ref}, Q_{ref}	Grid active and reactive reference powers
s_a, s_b, s_c	Switching state of the upper switch at each leg.
T_s	Sampling time.
AC	Alternating Current
ACVF	Alternating Current Variable Frequency
ATRU	Auto-Transformer Rectifiers Unit
ESR	Equivalent Series Resistance
EKF	Extended Kalman Filter
FCS-MPC	Finite Control Set-Model Predictive Control
IGBT	Insulated Gate Bipolar Transistor
LSE	Least Square Estimation
TRU	Transformer rectifiers Unit
THD	Total Harmonic Distortion
MPC	Model Predictive Control
MPDPC	Model Predictive Direct Power Control
PWM	Pulse Width Modulation
UPS	Uninterruptable Power Supply

Appendix

1. Bayesian Theorem and Multivariate Distribution

Bayesian estimation is a method of mathematically formalizing and using a priori information as a random variable with a known distribution $\pi(\theta)$, which is usually called the prior distribution of $\pi(\theta)$.

Assuming that the distribution density of population X is $p(x|\theta)$, since the prior distribution of θ is known, the distribution density of population X can be regarded as the conditional distribution density of X at a given θ. The distribution density of population X is changed to $p(x|\theta)$.

Assuming that $X = (X_1, \cdots\cdots X_n)^T$ is a sample taken from the X. When a given sample value= $(X_1, \cdots\cdots X_n)^T$, the joint density (or the likelihood function) is

$$q(x|\theta) = \prod_{i=1}^{n} p(x_i|\theta) \tag{A1}$$

Thus, the joint probability distribution of sample X and parameter θ is

$$f(x, \theta) = q(x|\theta)\pi(\theta) \tag{A2}$$

By the total probability formula, (2) is transformed to the following equation.

$$f(x, \theta) = q(x|\theta)\pi(\theta) = m(x)h(\theta|x) \tag{A3}$$

$$h(\theta\Big|x) = \frac{q(x|\theta)\pi(\theta)}{m(x)} \quad \text{(A4)}$$

At a given sample X = x, $h(\theta|x)$ is called the posterior distribution of θ, which is also the conditional distribution of θ. The$m(x)$ in (4) is expressed as a prior distribution of the sample X. Because $m(x)$ does not depend on theta, if $m(x)$ is omitted, the Bayesian formula can be written as the following equivalent form.

$$\mathrm{h}(\theta|x) \propto q(x|\theta)\pi(\theta) \quad \text{(A5)}$$

where the symbol "∝" indicates that there is only one constant factor independent of θ on both sides. The right-hand side of (5) is not a normal distribution density function but it is the main part of the posterior distribution $h(\theta|x)$, called the kernel of $h(\theta|x)$.

For the multivariate variable $Z = (z_1, \cdots\cdots, z_n)$, if its distribution density is

$$f(z_1, \ldots\ldots, z_n) = (2\pi)^{-n/2}\left|\Sigma^{-1}\right|^{1/2} \exp\{-\frac{1}{2}[z-\mu]'\Sigma^{-1}[z-\mu]\} \quad \text{(A6)}$$

Then Z is subject to multivariate normal distribution and is written as $Z \sim N_n(\mu, \Sigma)$.

2. Bayesian estimation with the MPDPC for PWM rectifiers

In Bayesian estimation, there is a distribution of probabilities for any event. In (15), the sampling T_s frequency is known. Suppose R_s, L_s and v are normal distributions and independent of each other. The Bayesian estimation method is used to estimate the actual values of R_s, L_s and v at time instant k.

$$\begin{array}{c} R_s \sim N(r, \Sigma_r) \\ L_s \sim N(L, \Sigma_L) \\ v \sim N(0, \Sigma_v) \end{array} \quad \text{(A7)}$$

It is assumed that the measured interferences $\varepsilon_1, \cdots\cdots, \varepsilon_{k-1}$ follow the multivariate normal distribution and are independent and identically distributed.

$$\varepsilon_{(j)} \sim N_m(0, \Sigma_\varepsilon) \quad \text{(A8)}$$

For (8), as the j row of the measurement error vector, ε is denoted by $\varepsilon_{(j)}$, $\mathrm{Y}_{(j)}$ can be expressed as:

$$\mathrm{Y}_{(j+1)} \sim N_m\Big((\Phi\theta)_{(j)}, \Sigma\Big) \quad \text{(A9)}$$

Therefore, $\mathrm{Y}_{(2)}, \cdots\cdots, \mathrm{Y}_{(k)}$ are also independent of each other and obey multivariate normal distribution. For (15), the output matrix Y likelihood function is derived as shown below:

$$\mathrm{L}(\mathrm{Y}, \Phi|\theta, \Sigma) = (2\pi)^{-(k-1)/2}\left|\Sigma^{-1}\right|^{(k-1)/2} \bullet \exp\left\{-\frac{1}{2}tr[\mathrm{Y}-(\Phi\theta)]'[\mathrm{Y}-(\Phi\theta)]\Sigma^{-1}\right\} \quad \text{(A10)}$$

where Σ denotes the covariance matrix of the measurement error. The (10) is transformed through mathematical equation.

$$\mathrm{L}(\mathrm{Y}, \Phi|\theta, \Sigma) = \frac{\left|\Sigma^{-1}\right|^{3/2}}{(2\pi)^{-(k-1)/2}} \exp\left\{-\frac{1}{2}tr(\theta-\hat{\theta})'\Phi'\Phi(\theta-\hat{\theta})\Sigma^{-1}\right\} \cdot \left|\Sigma^{-1}\right|^{(k-4)/2} \exp\left\{-\frac{1}{2}trS\Sigma^{-1}\right\} \quad \text{(A11)}$$

where

$$\begin{array}{c} \hat{\theta} = (\Phi'\Phi)^{-1}\Phi'\mathrm{Y} \\ S = [\mathrm{Y}-(\Phi\hat{\theta})]'[\mathrm{Y}-(\Phi\hat{\theta})] \end{array} \quad \text{(A12)}$$

According to the assumption that R_s, L_s and v are normal and independent, the a priori distribution of the coefficient θ obeys the multivariate normal distribution as follows:

$$h(\theta|\Sigma^{-1}) \propto \left|\Sigma^{-1}\right|^{3/2} \exp\left\{-\frac{1}{2}tr(\theta-\mu_0)'\mathrm{E}(\theta-\mu_0)\Sigma^{-1}\right\} \quad \text{(A13)}$$

where μ_0 denotes the expectation of the coefficient θ and E denotes the identity matrix.

According to the Bayesian theorem, the posterior distribution of θ can be expressed as the product of the likelihood function and the prior distribution.

$$h(\theta,\Sigma^{-1}|\Phi,\mathrm{Y}) \propto h(\theta\left|\Sigma^{-1}\right.)\bullet L(\Phi,\mathrm{Y}\left|\theta,\Sigma^{-1}\right.) \propto \left|\Sigma^{-1}\right|^{(k+2)/2}\exp\left\{-\frac{1}{2}tr\left[(\theta-\overset{*}{\theta})'(\mathrm{E}+\Phi'\Phi)(\theta-\overset{*}{\theta})\right]\Sigma^{-1}\right\} \quad \text{(A14)}$$

where

$$\overset{*}{\theta} = (A+\Phi'\Phi)^{-1}(E\mu_0+\Phi'\Phi\hat{\theta}) = (E+\Phi'\Phi)^{-1}(\mu_0+\Phi'\Phi\hat{\theta}) \quad \text{(A15)}$$

(15) shows the posterior distribution of θ, which indicates that the posterior distribution of θ also obeys multivariate normal distribution, that is

$$h(\theta|\Phi,\mathrm{Y}) \sim MN_{3\times 1}[\overset{*}{\theta},\Sigma\otimes(\mathrm{E}+\Phi'\Phi)^{-1}] \quad \text{(A16)}$$

Thus, the expectation of the posterior distribution of θ is $\overset{*}{\theta}$, which is the Bayesian estimate of θ.

$$\hat{\theta}_B = \overset{*}{\theta} = (\mathrm{E}+\Phi'\Phi)^{-1}(\mu_0+\Phi'\Phi\hat{\theta}) = (\mathrm{E}+\Phi'\Phi)^{-1}(\mu_0+\Phi'\mathrm{Y}) \quad \text{(A17)}$$

References

1. Rodríguez, J.; Cortes, P. *Predictive Control of Power Converters and Electrical Drives*, 1st ed.; Wiley-IEEE Press: New York, NY, USA, 2012.
2. ParvezAkter, M.; Mekhilef, S.; Tan, M.L.N.; Akagi, H. Modified Model Predictive Control of a Bidirectional AC–DC Converter Based on Lyapunov Function for Energy Storage Systems. *IEEE Trans. Ind. Electron.* **2016**, *63*, 704–715. [CrossRef]
3. Antoniewicz, P.; Kazmierkowski, M.P. Virtual-Flux-Based Predictive Direct Power Control of AC/DC Converters with Online Inductance Estimation. *IEEE Trans. Ind. Electron.* **2008**, *55*, 4381–4390. [CrossRef]
4. Tokić, A.; Jukan, A.; Smajić, J. Parameter Estimation of Single-Phase Rectifier-Based Loads: Analytical Approach. *IEEE Trans. Power Deliv.* **2016**, *31*, 532–540. [CrossRef]
5. Liu, Y.; Ge, B.; Abu-Rub, H. A model predictive control for low-frequency ripple power elimination of active power filter integrated single-phase quasi-Z-source inverter. In Proceedings of the 2017 IEEE International Conference on Industrial Technology (ICIT), Toronto, ON, Canada, 22–25 March 2017; pp. 1540–1545.
6. Park, J.M.; Lee, K.H.; Park, Y.J.; Lee, J.H.; Won, C.Y. Predictive control for single-phase multi-module UPS inverters with output LC filter modeling. In Proceedings of the 2017 20th International Conference on Electrical Machines and Systems (ICEMS), Sydney, NSW, Australia, 11–14 August 2017; pp. 1–6.
7. Eid, A.; EI-Kishky, H.; Abdel-Salam, M.; El-Mohandes, T. Power Quality Investigations of VSCF Aircraft Electric Power Systems. In Proceedings of the IEEE 42th South Eastern Symposium on System Theory University of Texas, Tyler, TX, USA, 7–9 March 2010; pp. 171–176.
8. Department of Defense. MIL-STD-704F Aircraft Electric Power Characteristics. Military Standard. Available online: https://prod.nais.nasa.gov/eps/eps_data/137899-SOL-001-015.pdf2004 (accessed on 12 March 2004).
9. Young, H.A.; Perez, M.A.; Rodriguez, J. Analysis of Finite-Control-Set Model Predictive Current Control with Model Parameter Mismatch in a Three-Phase Inverter. *IEEE Trans. Ind. Electron.* **2016**, *63*, 3100–3107. [CrossRef]
10. CortÉs, P.; RodrÍguez, J.; Antoniewicz, P.; Kazmierkowski, M. Direct Power Control of an AFE Using Predictive Control. *IEEE Trans. Power Electron.* **2008**, *23*, 2516–2523. [CrossRef]
11. Kwak, S.; Park, J.C. Model-Predictive Direct Power Control with Vector Preselection Technique for Highly Efficient Active Rectifiers. *IEEE Trans. Ind. Inform.* **2015**, *11*, 44–52. [CrossRef]
12. Kahia, B.; Bouafia, A.; Abdelrahem, M.; Zhang, Z.; Chaoui, A.; Krama, A.; Kennel, R. A predictive direct power control strategy for three-level npc rectifier. In Proceedings of the 2017 5th International Conference on Electrical Engineering-Boumerdes (ICEE-B), Boumerdes, Algeria, 29–31 October 2017; pp. 1–5.
13. Cortes, P.; Rodriguez, J.; Silva, C.; Flores, A. Delay Compensation in Model Predictive Current Control of a Three-Phase Inverter. *IEEE Trans. Ind. Electron.* **2012**, *59*, 1323–1325. [CrossRef]

14. Léchappé, V.; Rouquet, S.; González, A.; Plestan, F.; León, J.D.; Moulay, E.; Glumineau, A. Delay Estimation and Predictive Control of Uncertain Systems with Input Delay: Application to a DC Motor. *IEEE Trans. Ind. Electron.* **2016**, *63*, 5849–5857. [CrossRef]
15. Kwak, S.; Moon, U.C.; Park, J.C. Predictive-Control-Based Direct Power Control with an Adaptive Parameter Identification Technique for Improved AFE Performance. *IEEE Trans. Power Electron.* **2014**, *29*, 6178–6187. [CrossRef]
16. Ma, J.; Song, W.; Wang, S.; Feng, X. Model Predictive Direct Power Control for Single Phase Three Level Rectifier at Low Switching Frequency. *IEEE Trans. Power Electron.* **2018**, *33*, 1050–1062. [CrossRef]
17. Wang, F.; Davari, S.A.; Chen, Z.; Zhang, Z.; Khaburi, D.A.; Rodríguez, J.; Kennel, R. Finite Control Set Model Predictive Torque Control of Induction Machine with a Robust Adaptive Observer. *IEEE Trans. Ind. Electron.* **2017**, *64*, 2631–2641. [CrossRef]
18. Xia, C.; Wang, M.; Song, Z.; Liu, T. Robust Model Predictive Current Control of Three-Phase Voltage Source PWM Rectifier with Online Disturbance Observation. *IEEE Trans. Ind. Inform.* **2012**, *8*, 459–471. [CrossRef]
19. Rubagotti, M.; Raimondo, D.M.; Ferrara, A.; Magni, L. Robust Model Predictive Control with Integral Sliding Mode in Continuous-Time Sampled-Data Nonlinear Systems. *IEEE Trans. Autom. Control* **2011**, *56*, 556–570. [CrossRef]
20. Yang, H.; Zhang, Y.; Liang, J.; Gao, J.; Walker, P.D.; Zhang, D. Sliding-Mode Observer Based Voltage-Sensorless Model Predicitve Power Control of PWM Rectifier Under Unbalanced Grid Conditions. *IEEE Trans. Ind. Electron.* **2018**, *65*, 5550–5560. [CrossRef]
21. Hoffmann, N.; Fuchs, F.W. Online grid impedance estimation for the control of grid connected converters in inductive-resistive distributed power-networks using extended kalman-filter. In Proceedings of the 2012 IEEE Energy Conversion Congress and Exposition (ECCE), Raleigh, NC, USA, 15–20 September 2012; pp. 922–929.
22. Ghanem, A.; Rashed, M.; Sumner, M.; Elsayes, M.A.; Mansy, I.I.I. Grid impedance estimation for islanding detection and adaptive control of converters. *IET Power Electron.* **2017**, *10*, 1279–1288. [CrossRef]
23. Rufa'I, N.A.; Zhang, L.; Chong, B. Performance analysis of adaptive notch filter active damping methods for grid-connected converters under a varying grid impedance. In Proceedings of the 2017 IEEE Manchester PowerTech, Manchester, UK, 18–22 June 2017; pp. 1–6.
24. Arif, B.; Tarisciotti, L.; Zanchetta, P.; Clare, J. Finite Set Model Predictive Control with a novel online grid inductance estimation technique. In Proceedings of the 7th IET International Conference on Power Electronics, Machines and Drives (PEMD 2014), Manchester, UK, 8–10 April 2014; pp. 1–6.
25. Yang, Y.; Hui, S.; Tan, S. Adaptive Reference Model Predictive Control for Power Electronics. In Proceedings of the 2016 IEEE Applied Power Electronics Conference and Exposition (APEC), Long Beach, CA, USA, 20–24 March 2016; pp. 1169–1175.
26. Ciobotaru, M.; Teodorescu, R.; Rodriguez, P.; Timbus, A.; Blaabjerg, F. Online grid impedance estimation for single-phase grid-connected systems using PQ variations. In Proceedings of the 2007 IEEE Power Electronics Specialists Conference, Orlando, FL, USA, 17–21 June 2007; pp. 2306–2312.
27. Rohten, J.A.; Espinoza, J.R.; Muñoz, J.A.; Sbarbaro, D.G.; Perez, M.A.; Melín, P.E.; Silva, J.J.; Espinosa, E.E. Enhanced Predictive Control for a Wide Time-Variant Frequency Enviroment. *IEEE Trans. Ind. Electron.* **2016**, *63*, 5827–5837. [CrossRef]
28. Akagi, H.; Kanazawa, Y.; Nabae, A. Instantaneous Reactive Power Compensators Comprising Switching Devices without Energy Storage Components. *IEEE Trans. Ind. Appl.* **1984**, *IA-20*, 625–630. [CrossRef]
29. Capua, G.D.; Femia, N. A Novel Method to Predict the Real Operation of Ferrite Inductors with Moderate Saturation in Switching Power Supply Applications. *IEEE Trans. Power Electron.* **2016**, *31*, 2456–2464. [CrossRef]
30. Rice, J. *Mathematical Statistics and Data Analysis*, 3rd ed.; Duxbury Press: Belmont, CA, USA, 1994.
31. Typhoon 600's Hard-in-Loop Platform User Manual, Typhoon HIL Inc., 2006. Available online: https://www.typhoon-hil.com/products/hil602 (accessed on 21 December 2016).